

# X-ray emission from the galaxies in Abell 2634

I. Sakelliou, M. R. Merrifield

*Department of Physics and Astronomy, University of Southampton, Southampton SO17 1BJ*

7 January 2018

## ABSTRACT

It is difficult to detect X-ray emission associated with galaxies in rich clusters because the X-ray images of the clusters are dominated by the emission from their hot intracluster media (ICM). Only the nearby Virgo cluster provides us with information about the X-ray properties of galaxies in clusters. Here we report on the analysis of a deep *ROSAT* HRI image of the moderately-rich cluster, Abell 2634, by which we have been able to detect the X-ray emission from the galaxies in the cluster. The ICM of Abell 2634 is an order of magnitude denser than that of the Virgo cluster, and so this analysis allows us to explore the X-ray properties of individual galaxies in the richest environment yet explored.

By stacking the X-ray images of the galaxies together, we have shown that their emission appears to be marginally resolved by the HRI. This extent is smaller than for galaxies in poorer environments, and is comparable to the size of the galaxies in optical light. These facts suggest that the detected X-ray emission originates from the stellar populations of the galaxies, rather than from extended hot interstellar media. Support for this hypothesis comes from placing the optical and X-ray luminosities of these galaxies in the  $L_B$ – $L_X$  plane: the galaxies of Abell 2634 lie in the region of this plane where models indicate that all the X-ray emission can be explained by the usual population of X-ray binaries. It is therefore probable that ram pressure stripping has removed the hot gas component from these galaxies.

**Key words:** galaxies: clusters: individual: A2634 – galaxies: interactions – intergalactic medium – X-rays: galaxies

## 1 INTRODUCTION

The advent of the *Einstein* observatory changed the belief that early-type galaxies contain little interstellar gas by revealing hot X-ray emitting halos associated with many of them (e.g. Forman et al. 1979). Subsequent X-ray observations led to the conclusion that these galaxies can retain large amounts (up to  $\sim 10^{11} M_\odot$ ) of hot ( $T \sim 10^7$  K) interstellar medium (Forman, Jones & Tucker 1985; Trinchieri & Fabbiano 1985; Canizares, Fabbiano & Trinchieri 1987).

However, this picture might be expected to be different for galaxies that reside near the centres of rich clusters of galaxies, since their properties must be affected by their dense environment. For example, we might expect interstellar medium (ISM) gas to be stripped from the galaxy by the ram pressure resulting from the passage of the galaxy through the intracluster medium (ICM) (Gunn & Gott 1972). Stripping of the ISM can also result from tidal interactions with other nearby galaxies (Richstone 1975; Merritt 1983, 1984). The most dramatic and well-studied example of a galaxy which appears to be in the process of being stripped of its ISM is the elliptical galaxy M86 in the Virgo cluster,

which shows a ‘plume’ of X-ray emission emanating from it (Forman et al. 1979; White et al. 1991; Rangarajan et al. 1995).

In addition to the mechanisms which remove the ISM of a galaxy, gas can also be replenished. The gravitational pull of a galaxy attracts the surrounding ICM. This gas ends up being concentrated in or behind the galaxy, depending on the velocity of the galaxy relative to the ICM (see, for example, Sakelliou, Merrifield & McHardy 1996). Stellar winds can also replenish the hot gas in a galaxy’s ISM.

All the processes mentioned above take place simultaneously. The relative importance of each process depends on: the galaxies’ velocities; the local density of the ICM; the number density of galaxies; their orbits in the cluster; and the gravitational potential of each galaxy. It is therefore *a priori* difficult to say which mechanism dominates in the cores of rich clusters of galaxies, and hence whether cluster galaxies are surrounded by the extensive X-ray emitting halos that we see associated with galaxies in the field.

Unfortunately, X-ray observations of rich clusters have generally not been of high enough quality to answer this

arXiv:astro-ph/9710092v1 9 Oct 1997

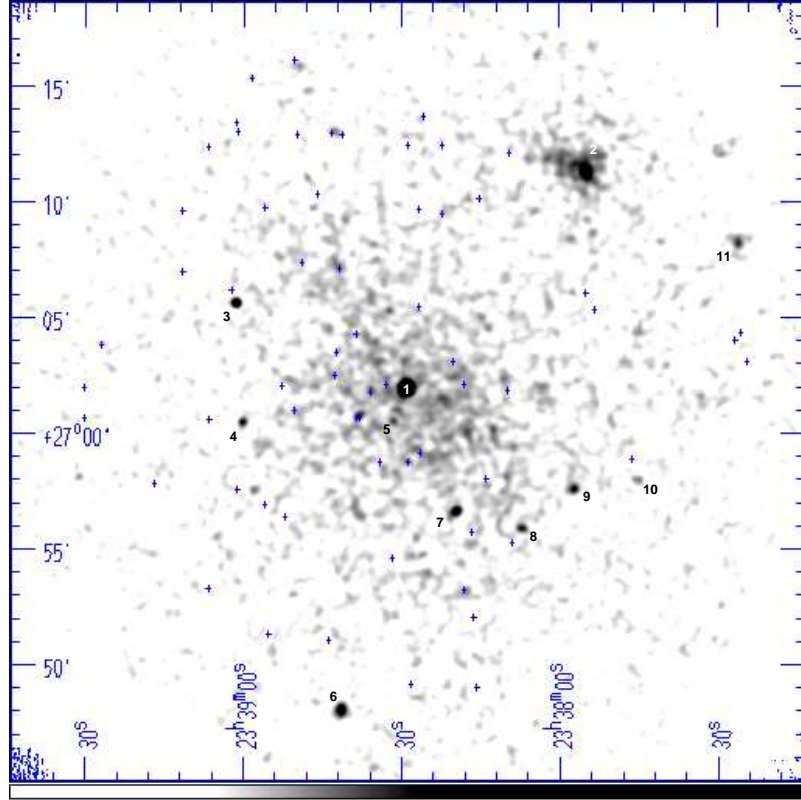


**Figure 1.** Grey-scale *ROSAT* HRI image of the core of the cluster Abell 2634. The image has been smoothed using a Gaussian kernel with a dispersion of 8 arcsec. The positions of the cluster galaxies with measured redshift are marked with crosses.

question, since any emission from the galaxies is hard to detect against the high X-ray background produced by the cluster’s ICM (Canizares & Blizzard 1991; Vikhlinin, Forman & Jones 1994; Bechtold et al. 1983; Grebenev et al. 1995; Soltan & Fabricant 1990; Mahdavi et al. 1996). In the cases where galaxy X-ray emission has been reported, the studies have been restricted to a few bright cluster galaxies, and it has not proved possible to investigate the general galaxy population in a statistically complete manner.

In order to search for X-ray emission from galaxies in a moderately rich environment, we obtained a deep *ROSAT* HRI observation of the core of the rich cluster Abell 2634, which is a nearby ( $z=0.0312$ ) centrally-concentrated cluster of richness class I. In §2.1 we describe the analysis by which the X-ray emission from the galaxies in this cluster was detected. In §2.2 we explore the properties of this X-ray emission, and show that the galaxies in this cluster lack the extensive gaseous halos of similar galaxies in poorer environments. In §3, we show how this difference can be attributed to ram pressure stripping.

## 2 X-RAY OBSERVATIONS AND ANALYSIS

The core of Abell 2634 was observed with the *ROSAT* HRI in two pointings, in January and June 1995, for a total of 62.5 ksec. The analysis of these data was performed with the IRAF/PROS software.

Inspection of the emission from the cD galaxy and other bright X-ray sources in the images from the two separate

observations indicates that the two sets of observations do not register exactly and that a correction to the nominal *ROSAT* pointing position is required. Therefore, the second set of observations was shifted by  $\sim 2.0$  arcsec to the east and  $\sim 0.8$  arcsec to the south; such a displacement is consistent with typical *ROSAT* pointing uncertainties (Briel et al. 1996). Both images were then registered with the optical reference frame to better than an arcsecond. A grey-scale image of the total exposure is shown in Fig. 1. The image has been smoothed with a Gaussian kernel of 8 arcseconds dispersion. At the distance of Abell 2634, 1 arcsec corresponds to 900 pc.\*

This deep image of Abell 2634 reveals the largescale X-ray emission from the hot ICM of the cluster and a few bright sources, which are numbered on Fig. 1. Source 1 is the cD galaxy NGC 7720, located near the centre of Abell 2634. It hosts the prototype wide-angle tailed radio source 3C 465 (e.g. Eilek et al. 1984). Source 2 is a background cluster at a redshift of  $cz \simeq 37,000 \text{ km s}^{-1}$  (Pinkney et al. 1993; Scodreggio et al. 1995). For the rest of the X-ray bright sources, the Automatic Plate Measuring machine, run by the Royal Greenwich Observatory in Cambridge, was used to obtain optical identifications. Table 1. gives the positions of these sources as determined from the X-ray image, and the class of their optical counterparts. The position of source 7 coincides with a faint object in the Palomar sky survey, but

\* Here, as throughout this paper, we have adopted a Hubble constant of  $H_0 = 50 \text{ km s}^{-1} \text{ Mpc}^{-1}$ .

**Table 1.** Bright Sources

Source	$\alpha$ (J2000) h m s	$\delta$ (J2000) ° ' "	ID/notes
1	23 38 29.1	27 01 53.5	cD galaxy
2	23 37 56.1	27 11 31.3	cluster
3	23 39 01.6	27 05 35.9	star
4	23 39 00.5	27 00 27.9	star
5	23 38 31.7	27 00 30.5	nothing
6	23 38 41.5	26 48 04.1	star
7	23 38 19.8	26 56 41.5	?
8	23 38 07.4	26 55 52.8	star
9	23 37 57.5	26 57 30.1	galaxy ?
10	23 37 45.3	26 57 53.1	two objects
11	23 37 26.2	27 08 14.6	?

there is also a nearby star, and source 11 does not seem to have a discernible optical counterpart. All these sources were masked out in the subsequent analysis.

The positions of galaxies that are members of Abell 2634 are also indicated on Fig. 1. Pinkney et al. (1993) collected the redshifts of  $\sim 150$  galaxies that are probable members Abell 2634 (on the basis that their redshifts lie in the range  $6,000 < cz < 14,000 \text{ km s}^{-1}$ ), and Scodreggio et al. (1995) have increased the number of galaxies whose redshifts confirm that they are cluster members up to  $\sim 200$ . The sample of redshifts is complete to a magnitude limit of 16.5, and from this magnitude-limited sample we have selected those galaxies that appear projected within a circle of 15 arcmin radius, centered on the cD galaxy. This selection yields 62 galaxies, of which the vast majority are of type E and S0 – only 10 are classified as spirals or irregular. The positions of these galaxies are taken from the CCD photometry of Pinkney (1995) and Scodreggio et al. (1995), and are accurate to  $\sim 1$  arcsec. They are marked as crosses on Fig. 1.

Inspection of Fig. 1 reveals several cases where the location of a galaxy seems to coincide with an enhancement in the cluster’s X-ray emission, and it is tempting to interpret such enhancements as the emission from the galaxy’s ISM. However, it is also clear from Fig. 1 that the X-ray emission in this cluster contains significant small-scale fluctuations and non-uniformities. We must therefore consider the possibility that the apparent associations between galaxy locations and local excesses in the X-ray emission may be chance superpositions. We therefore now present a more objective approach to searching for the X-ray emission from cluster galaxies.

## 2.1 Detection of the cluster galaxies

Before adopting an approach to detecting the emission from cluster galaxies, we must first have some notion as to how bright we might expect the emission to appear in this deep HRI image. Previous X-ray observations have shown that the X-ray luminosities of E and S0 galaxies in the 0.2-3.5 keV energy band range from  $\sim 10^{39}$  to  $\sim 10^{42} \text{ erg s}^{-1}$  (Kim, Fabbiano & Trinchieri 1992a, b; Forman et al. 1985). These limits at the distance of Abell 2634 correspond to fluxes of  $5 \times 10^{-16}$  to  $5 \times 10^{-13} \text{ erg s}^{-1} \text{ cm}^{-2}$ . We have used the PIMMS software to convert these limits to count rates for the *ROSAT* HRI detector. The emission from the galax-

ies was modeled by a Raymond-Smith plasma (Raymond & Smith 1977) with a temperature  $kT = 0.862 \text{ keV}$  and a metal abundance of 25% solar; these quantities are consistent with the values previously found from observations of early-type galaxies (Kim et al. 1992a; Matsushita et al. 1994; Awaki et al. 1994). The absorption by the galactic hydrogen was also taken into account by using the column density given by Stark et al. (1992) for the direction of Abell 2634 ( $N_{\text{H}} = 4.94 \times 10^{20} \text{ cm}^{-2}$ ). These calculations predict that the 62.5 ksec HRI observation of this cluster should yield somewhere between  $\sim 1$  and  $\sim 1200$  counts from each galaxy. Motivated by this prediction of a respectable, but not huge, number of counts per galaxy, we set out to detect emission associated with cluster galaxies.

We are trying to detect this fairly modest amount of emission against the bright background of the ICM emission. We therefore seek to improve the statistics by stacking together the X-ray images in the vicinity of the 40 E and S0 galaxies marked in Fig. 1. Fig. 2. presents a contour plot of the combined image, which covers a region of 1 arcmin radius around the stacked galaxies. The centre of the plot coincides with the optical centres of the individual galaxies. Clearly, there appears to be X-ray emission associated with the cluster galaxies, and it is centered at their optical positions. This coincidence provides us with some confidence that the X-ray and optical frames are correctly registered. We have also constructed a composite brightness profile for the 40 galaxies by adding the unsmoothed counts detected in concentric annuli centered on each galaxy. The width of each annulus in this profile was set at 6 arcsec and the local background, as measured in an annulus between 1.0 and 2.0 arcmin around each galaxy, was subtracted. The resulting profile is presented in Fig. 3. Once again, the excess of emission in the vicinity of the cluster galaxies is apparent.

In order to assess the significance of this detection, we generated 100 sets of simulated data from randomly selected points on the image. The diffuse emission from the ICM varies systematically with radius, and so we might expect the probability that a galaxy is coincidentally aligned with a clump in the ICM emission to vary systematically with radius. Further, the sensitivity of the HRI varies with radius, and so the detectability of the emission from a single galaxy will vary with radius as well. We therefore constructed the simulated data sets by extracting counts from the HRI image at the same radii as the true galaxy locations, but at randomized azimuthal angles. The mean profile and the RMS fluctuations amongst the simulated data sets are shown in Fig. 3. As might be expected, the average number of counts in these random data sets is zero; the larger RMS error bars at small radii reflect the smaller sizes of these annuli. From a  $\chi^2$  comparison between the observed galaxy profile and the simulated profile, we can conclude that there is less than 0.1% probability that the apparent peak in the galaxy emission is produced by chance. Thus, the detection of emission from the galaxies in Abell 2634 is highly statistically significant.

## 2.2 Origin of the X-ray emission

As mentioned in the introduction, early-type galaxies have been found to retain large amounts of hot gas, which extends far beyond the optical limits of the galaxies. X-ray binaries

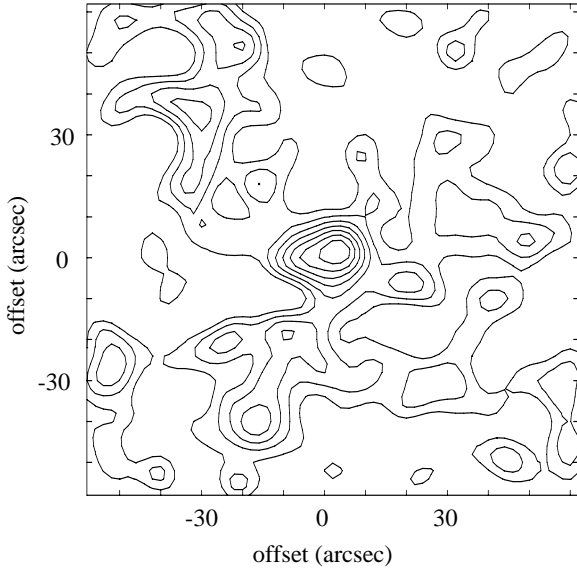


**Figure 2.** Contour plot of the combined image of all the early-type galaxies that belong to Abell 2634. The pixel size of the image is 2 arcsec and it has been smoothed with a Gaussian kernel of 2 pixels. The center of the plot coincides with the optical centres of the galaxies. The contour lines are from 20 to 100 per cent the peak value and are spaced linearly in intervals of 5 per cent.

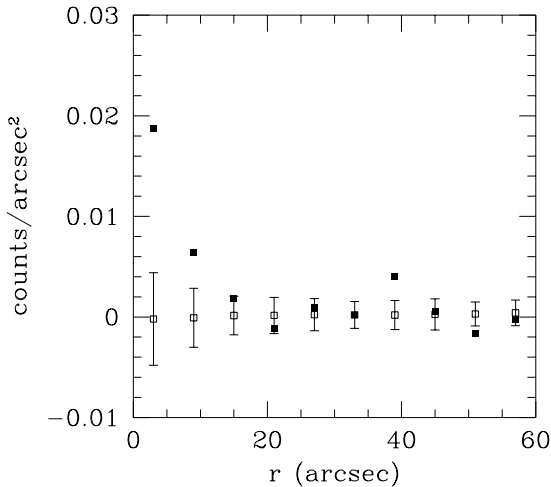


**Figure 3.** The combined surface brightness profile of all the early-type galaxies (filled squares) normalized to one galaxy. Open squares represent the average profile from the simulations.

also contribute to the total emission, and they become more dominant in X-ray faint galaxies. We might also expect some of the emission to originate from faint active galactic nuclei (AGNs) in the cores of these galaxies. Although none of the galaxies in our sample has been reported as an active galaxy, there is increasing dynamical evidence that the vast majority of elliptical galaxies contain central massive black holes (van der Marel et al. 1997; Kormendy et al. 1996a, 1996b; for a review Kormendy & Richstone 1995), and so

we might expect some contribution from low-level activity in such systems. We therefore now see what constraints the observed X-ray properties of the galaxies in Abell 2634 can place on the origins of the emission.

### 2.2.1 The extent of the X-ray emission

One diagnostic of the origins of the X-ray emission is the measurement of its spatial extent. AGN emission should be unresolved by the HRI, while emission from X-ray binaries should be spread over a similar spatial scale as the optical emission, and halos of hot gas should be still more extended.

In order to assess the spatial extent of the X-ray emission, we need to characterize the PSF in this HRI observation. The point sources detected in these data are more extended than the model PSF for the HRI detector given by Briel et al. (1996) as is seen in Fig. 4, where four of the sources are fitted by this model PSF (dash line). This discrepancy can be attributed to residual errors in the reconstruction of *ROSAT*'s attitude, which broaden the PSF in long integrations. We have therefore empirically determined the PSF that is appropriate for this observation by fitting the profiles of the point sources with a Gaussian PSF model (Fig. 4, solid line). Only sources 1, 3, 4, 8 are used for the determination of the width of the Gaussian. Source 6 is very elongated and can not be represented by a symmetrical function. The mean dispersion of the best-fit model was found to be  $(4.1 \pm 0.1)$  arcsec. All of the point sources detected in this image have widths consistent with this value, and so there is no evidence that the PSF varies with radius. We therefore adopt this PSF for the emission from all the galaxies in the observation.

Figure 5 shows the comparison between the adopted PSF and the emission from the cluster galaxies. The emission appears to be more extended than the PSF; fitting the data to the PSF yields a  $\chi^2$  value of 14.2 with 9 degrees of freedom, which is marginally consistent with the emission being unresolved. We can obtain a better fit by modeling the radial profile of the emission using a Gaussian, which we convolve with the PSF to model the observed profile. Fitting this model to the observations, we find that the intrinsic width of the X-ray emission is  $4.3^{+2.2}_{-2.8}$  arcsec. The best-fit model is also shown in Fig. 5.

The radius of the X-ray halos of early-type galaxies with optical luminosities comparable to those in this cluster has been shown to be  $\sim 20 - 60$  kpc (e.g. Fabbiano et al. 1992), with the lower values characterizing optically fainter galaxies. At the distance of Abell 2634 these values correspond to  $\sim 20 - 60$  arcsec, much larger than the upper limit of  $\sim 7$  arcsec we found for the extent of the galactic X-ray emission. Thus, the X-ray emission from the cluster galaxies, although apparently extended, clearly does not originate from the large halos of hot gas found around comparable galaxies in poorer environments.

One possible explanation for the spatial extent of the emission from these galaxies is that it could arise from errors in the adopted positions for the galaxies. Such errors would broaden the distribution of X-rays when the data from different galaxies are co-added even if the individual sources are unresolved. However, the zero-point of the X-ray reference frame is well tied-down by the detected point sources in the field. Further, the optical locations of the galaxies come

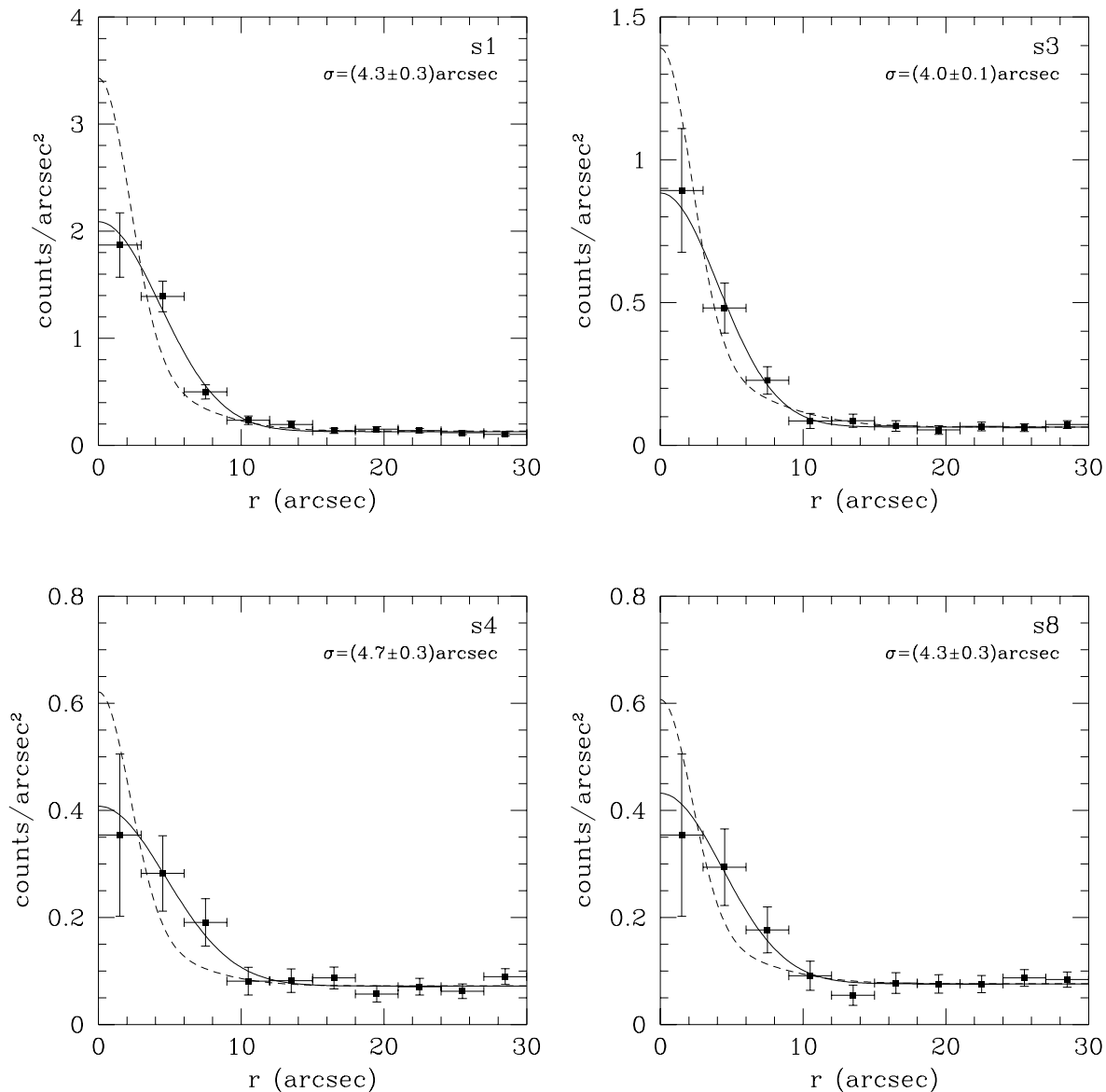


**Figure 4.** Surface brightness distribution of the bright sources in the HRI image. (s1, s3, s4, and s8). Source 1 is the central cD galaxy. The profile is fitted by the appropriate HRI PSF for the distance of the point source from the centre of the image (dash line) and a Gaussian (solid line). The calculated width ( $\sigma$ ) of the best fit Gaussian is also given.

from CCD photometry with positional errors of less than an arcsecond. It therefore cannot explain the  $\sim 4$  arcsec extent of the observed X-ray emission.

We therefore now turn to the extent of the X-ray emission that we might expect from X-ray binaries. Nearly half of the early-type galaxies that we use for our analysis have been imaged in the I-band by Scodreggio, Giovanelli & Haynes (1997). They have fitted the optical galaxy profile with a de Vaucouleur law, and found a mean value for their effective radii of  $\sim 8$  arcsec, with only 4 galaxies smaller than 3 arcsec and another 3 larger than 13 arcsec. These values are directly comparable to the spatial extent of the X-ray emission derived above. Thus, it would appear that the ob-

servations are consistent with what we would expect if the X-ray emission from the galaxies in Abell 2634 originates from X-ray binaries in these systems, although we have not ruled out the possibility that some fraction of the emission comes from AGN.

### 2.2.2 The luminosity of the X-ray emission

A further test of the origins of the X-ray emission in the cluster galaxies comes from its luminosity. It has been found that the blue luminosities of galaxies correlates with their X-ray luminosities, with the optically brighter galaxies being more luminous in X-rays (e.g. Forman et al. 1985; Fabbiano et

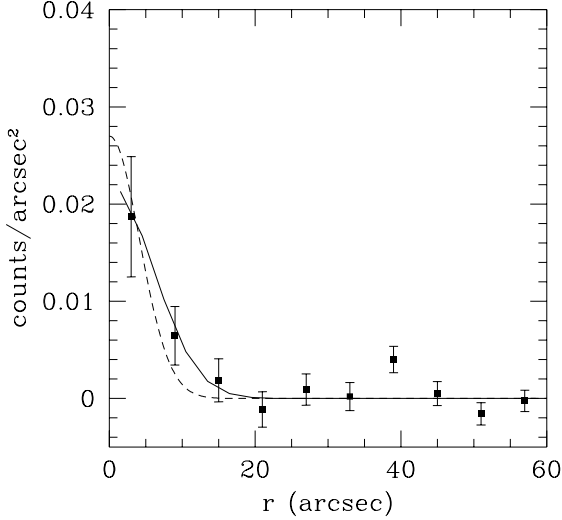


**Figure 5.** The combined surface brightness distribution of the 40 early-type galaxies, normalized to one galaxy. The profile is fitted by the measured HRI PSF (dashed line) and the spatially-extended model (solid line).

al. 1992). This correlation for the early-type galaxies in the Virgo cluster is presented in Fig. 6. The optical and X-ray luminosities of these galaxies are taken from Fabbiano et al. (1992). The line in this plot divides the  $L_B - L_X$  plane into two distinct galaxy types (Fabbiano & Schweizer 1995). In addition to the differences in the ratio of X-ray-to-optical luminosities, galaxies in these two regions have been shown to possess different spectral properties. The spectra of the X-ray bright galaxies [group (I)] are well fitted by Raymond-Smith models of 1 keV temperature, and it is believed that these galaxies retain large amounts of hot ISM. In the spectra of the X-ray faint galaxies of group (II), on the other hand, a hard component is present; X-ray binaries are believed to be the major source of the X-rays in these galaxies.

In order to see where the galaxies of Abell 2634 lie in this plot, we must calculate their optical and X-ray luminosities. Butcher & Oemler (1985) have measured  $J$  and  $F$  optical magnitudes for a large number of galaxies in Abell 2634. We have converted these magnitudes to the blue band by applying the colour relations provided by Oemler (1974) and Butcher & Oemler (1985), correcting for galactic extinction, and using the appropriate K-correction. We find that the absolute blue magnitude of the galaxies in the HRI image lie in the range from  $-18.5$  to  $-21.4$ . We have divided these galaxies into three groups according to their optical luminosities: group A  $(0.4 - 2.0) \times 10^{10} L_\odot$  with 17 galaxies; group B  $(2.1 - 3.7) \times 10^{10} L_\odot$  with 8 galaxies; and group C  $(3.8 - 5.5) \times 10^{10} L_\odot$  with only 2 galaxies.

The X-ray luminosity of each group was obtained by repeating the analysis of §2.1 using just the galaxies in each sub-sample. Using the PIMMS software we converted the observed count rate from the HRI image to X-ray luminosity in the energy range 0.2-3.5 keV. The thermal model used for the conversion is the same that was used by Fabbiano et al. (1992) to derive the plot shown in Fig. 6, and is discussed in §2.1.

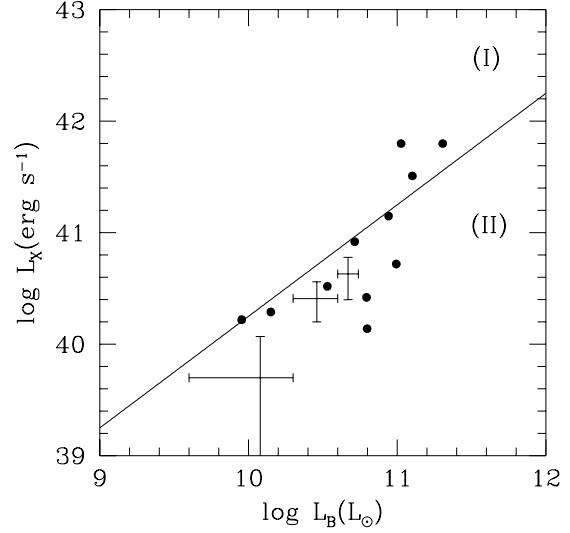


**Figure 6.** X-ray luminosity versus blue luminosity for the early-type galaxies. The line delineates the boundary between the locations of galaxies where the hot ISM makes a significant contribution to the total emission [region (I)], and the locations of galaxies where the entire emission can be ascribed to X-ray binaries [region (II)]. The locations in this plane of galaxies that belong to the Virgo cluster are marked by filled circles. The average properties of galaxies in Abell 2634 lying in different optical luminosity ranges are indicated by crosses.

The resulting values for optical and X-ray luminosities in each sub-sample are shown in Fig. 6. The horizontal error bars represent the width of each optical luminosity bin and the vertical ones show the errors in the measured X-ray luminosities. This plot shows that the galaxies in our sample follow the established correlation: the optically-brighter galaxies are also more luminous in the X-rays. The existence of this correlation also implies that the detected X-ray flux from the galaxies in Abell 2634 is not dominated by a few bright galaxies, but that the optically-fainter galaxies also contribute to the detected X-ray emission.

The galaxies in Abell 2634 probe the fainter end of the  $L_B - L_X$  relation as covered by Virgo galaxies. It should be borne in mind that there is a bias in the Virgo data which means that the two data sets in Fig. 6 are not strictly comparable. At the lower flux levels, a large number of Virgo galaxies have not been detected in X-rays, and so this plot preferentially picks out any X-ray-bright Virgo galaxies. For the Abell 2634 data, on the other hand, the co-addition of data from all the galaxies in a complete sample means that the data points represent a true average flux. However, it is clear that the X-ray fluxes from galaxies in these two clusters are comparable.

The similarity between the X-ray properties of galaxies in these two clusters is of particular interest because their environments differ significantly. The galaxies from the Virgo cluster shown in Fig. 6 lie in a region between 360 kpc and 2 Mpc from the centre of the cluster. Recent *ROSAT* PSPC observations have shown that the number density of the hot ICM of this cluster drops from  $3 \times 10^{-4}$  to  $3 \times 10^{-5} \text{ cm}^{-3}$  in this region (Nulsen & Böhringer 1995). The galaxies from

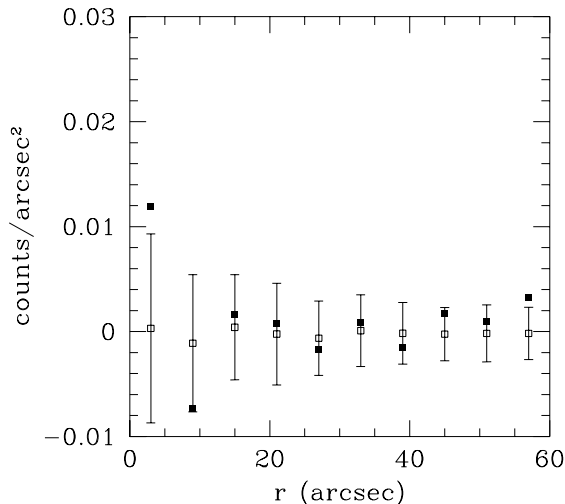


**Figure 7.** The combined surface brightness profile of the spiral galaxies that lie in the field of view of the HRI (filled squares) normalized to one galaxy. Open squares represent the average profile from the simulations.

Abell 2634 that have gone into this plot lie in the inner 0.8 Mpc of Abell 2634, and in this region the number density of the ICM varies between  $1 \times 10^{-3}$  and  $2 \times 10^{-4} \text{ cm}^{-3}$  (Sakelliou & Merrifield 1997). Thus, the galaxies in the current analysis come from a region in which the intracluster gas density is, on average, an order of magnitude higher than surrounding the Virgo cluster galaxies.

The location of the galaxies in region (II) of Fig. 6 adds weight to the tentative conclusion of the previous section that the X-ray emission from these galaxies can be explained by their X-ray binary populations, since any significant ISM contribution would place them in region (I). Similarly, the low X-ray fluxes of these galaxies leaves little room for a significant contribution from weak AGN. If the X-ray binary populations are comparable to those assumed by Fabbiano & Schweizer (1995) in calculating the dividing line in Fig. 6, then essentially all the X-ray emission from these galaxies can be attributed to the X-ray binaries. Thus, any average AGN emission brighter than a few times  $10^{40} \text{ erg s}^{-1}$  can be excluded, as such emission would also move the galaxies into region (I) of the  $L_B - L_X$  plane.

### 2.3 Spiral galaxies

Having discussed the X-ray properties of the early-type galaxies in Abell 2634 at some length, we now turn briefly to the properties of the spiral galaxies in the cluster. Abell 2634 is a reasonably rich system, and we therefore do not expect to find many spiral galaxies within it. Indeed, only 7 of the 62 galaxies whose redshifts place them at the distance of Abell 2634, and which lie within the field of the HRI, have been classified as spirals. The statistics are correspondingly poor when the X-ray emission around these galaxies is co-added: the combined profile is shown in Fig. 7, together with the results from the control simulations (see §2.1 for

details). It is clear from this figure that the spirals have not been detected in this observation, and a  $\chi^2$  fit confirms this impression.

The failure to detect these galaxies is not surprising. Not only are there relatively few of them, but their X-ray luminosities are lower than those of early-type galaxies. In the *Einstein* energy band (0.2 - 3.5 keV), their luminosities have been found to lie in the range  $\sim 10^{38}$  to  $\sim 10^{41} \text{ erg s}^{-1}$  (Fabbiano 1989). Modeling this emission using a Raymond-Smith model with a higher temperature than for the early-type galaxies, as appropriate for spiral galaxies (Kim et al. 1992a), we find that the expected count rate for these galaxies is a factor of  $\sim 40$  lower than for the ellipticals in the cluster. It is therefore unsurprising that we fail to detect the small number of spiral galaxies present in the cluster.

## 3 DISCUSSION

In this paper, we have detected the X-ray emission from the normal elliptical galaxies in Abell 2634. The limited spatial extent of this emission coupled with its low luminosity is consistent with it originating from normal X-ray binaries in the galaxies' stellar populations. These galaxies do not seem to have the extended hot ISM found around galaxies that reside in poorer cluster environments. We therefore now discuss whether this difference can be understood in terms of the physical processes outlined in the introduction.

Intuitively, the simplest explanation for the absence of an extensive halo around a cluster galaxy is that it has been removed by ram pressure stripping as the galaxy travels through the ICM. A simple criterion for the efficiency of this process can be obtained by comparing the gravitational force that holds the gas within the galaxy to the force due to the ram pressure, which tries to remove it (Gunn & Gott 1972).

The gravitational force is given by:

$$F_{\text{GR}} \sim G \frac{M_{\text{gal}} M_{\text{gas}}}{R_{\text{gal}}^2} \quad (1)$$

where  $M_{\text{gal}}$  is the total mass of the galaxy,  $M_{\text{gas}}$  is the mass of the X-ray emitting gas, and  $R_{\text{gal}}$  is the radius of the galaxy's X-ray halo. For typical values for the masses of the galaxy and the gas of  $10^{12} M_{\odot}$  (Forman et al. 1985) and  $5 \times 10^9 M_{\odot}$  (e.g. Canizares et al. 1987) respectively, and a mean value for  $R_{\text{gal}}$  of 40 kpc (Canizares et al. 1986), which is a representative value for galaxies of the same optical luminosity as the galaxies in Abell 2634, equation (1) implies that  $F_{\text{GR}} \sim 1 \times 10^{30} \text{ N}$ .

The force due to ram pressure is described by:

$$F_{\text{RP}} = \rho_{\text{ICM}} v_{\text{gal}}^2 \pi R_{\text{gal}}^2 = \mu m_{\text{p}} n v_{\text{gal}}^2 \pi R_{\text{gal}}^2 \quad (2)$$

where  $\rho_{\text{ICM}}$  is the density of the ICM,  $\mu$  is the mean molecular weight,  $m_{\text{p}}$  is the proton mass,  $n$  is the number density of the ICM, and  $v_{\text{gal}}$  is the galaxy velocity. From the velocity dispersion profile of Abell 2634 presented by den Hartog & Katgert (1996) we find that the velocity dispersion,  $\sigma_v$ , in the inner 15 arcmin of this system is  $\approx 710 \text{ km s}^{-1}$ . Assuming an isotropic velocity field, the characteristic three-dimensional velocity of each galaxy is hence  $v_{\text{gal}} = \sqrt{3} \sigma_v \approx 1230 \text{ km s}^{-1}$ . The number density of the ICM in the same inner region has been derived from recent

*ROSAT* PSPC data (Schindler & Prieto 1997) and this HRI observation (Sakelliou & Merrifield 1997), and is found to vary from  $1 \times 10^{-3} \text{ cm}^{-3}$  down to  $2 \times 10^{-4} \text{ cm}^{-3}$ , consistent with previous *Einstein* observations (Jones & Forman 1984; Eilek et al. 1984). Inserting these values into equation (2), we find  $F_{\text{RP}} \sim (1 - 10) \times 10^{30} \text{ N}$ .

Thus, the ram pressure force exerted on the galaxies in Abell 2634 is found to be larger than the force of gravity, and so we might expect ram pressure stripping to be an effective mechanism for removing the ISM from these galaxies. In poorer environments, the density of the ICM is likely to be at least a factor of ten lower, and the velocities of galaxies will be a factor of  $\sim 3$  smaller. We might therefore expect  $F_{\text{RP}}$  to be a factor of  $\sim 100$  lower in poor environments. Since such a change would make  $F_{\text{RP}} < F_{\text{GR}}$ , it is not surprising that galaxies in poor environments manage to retain their extensive halos.

The absence of extensive X-ray halos around the galaxies in Abell 2634 implies that ram pressure stripping dominates the processes of accretion and stellar mass loss which can replenish the ISM. By carrying out similar deep X-ray observations of clusters spanning a wide range of ICM properties, it will be interesting to discover more precisely what sets of physical conditions can lead to the efficient ISM stripping that we have witnessed in Abell 2634.

## ACKNOWLEDGEMENTS

We are indebted to the referee, Alastair Edge, for a very insightful report on the first incarnation of this paper. We thank Jason Pinkney for providing us with the positions and redshifts of the galaxies and Rob Olling for helpful discussions. This research has made use of the NASA/IPAC Extragalactic Database (NED) which is operated by the Jet Propulsion Laboratory, California Institute of Technology, under contract with the National Aeronautics and Space Administration. Much of the analysis was performed using IRAF, which is distributed by NOAO, using computing resources provided by STARLINK. MRM is supported by a PPARC Advanced Fellowship (B/94/AF/1840).

## REFERENCES

- Awaki H., Mushotzky R., Tsuru T., Fabian A. C., Fukazawa Y., Loewenstein M., Makishima K., Matsumoto H., Matsushita K., Mihara T., Ohashi T., Ricker G. R., Serlemitsos R. J., Tsusaka Y., Yamazaki T., 1994, PASJ, 46, L65
- Bechtold J., Forman W., Giacconi R., Jones C., Schwarz J., Tucker W., Van Speybroeck L., 1983, ApJ, 265, 26
- Briel et al. 1996, *ROSAT* Handbook
- Butcher H. R., Oemler A. JR., 1985, ApJS, 57, 665
- Canizares C. R., Blizzard P., 1991, ApJ, 382, 79
- Canizares C. R., Donahue M. E., Trinchieri G., Stewart G. C., McGlynn T. A., 1986, ApJ, 304, 312
- Canizares C. R., Fabbiano G., Trinchieri G., 1987, ApJ, 312, 503
- den Hartog R., Katgert P., 1996, MNRAS, 279, 349
- Eilek J. A., Burns J. O., O'Dea C. P., Owen F. N., 1984, ApJ, 278, 37
- Fabbiano G., 1989, ARA&A, 27, 87
- Fabbiano G., Schweizer F., 1995, ApJ, 447, 572
- Fabbiano G., Kim D.-W., Trinchieri G., 1992, ApJS, 80, 531
- Forman W., Jones C., Tucker W., 1985, ApJ, 293, 102
- Forman W., Schwarz J., Jones C., Liller W., Fabian A. C., 1979, ApJ, 234, L27
- Grebenev S. A., Forman W., Jones C., Murray S., 1995, ApJ, 607
- Gunn J. E., Gott J. R., 1972, ApJ, 176, 1
- Jones C., Forman W., 1984, ApJ, 276, 38
- Kim D.-W., Fabbiano G., Trinchieri G., 1992a, ApJS, 80, 645
- Kim D.-W., Fabbiano G., Trinchieri G., 1992b, ApJ, 393, 134
- Kormendy J., Richstone D., 1995, ARA&A, 33, 581
- Kormendy J., Bender R., Ajhar E. A., Dressler A., Faber S. M., Gebhardt K., Grillmair C., Lauer T. R., Richstone D., Tremaine S., 1996a ApJL, 473, 91
- Kormendy J., Bender R., Ajhar E. A., Dressler A., Faber S. M., Gebhardt K., Grillmair C., Lauer T. R., Richstone D., Tremaine S., 1996b ApJL, 459, 57
- Mahdavi A., Geller M. J., Fabricant D. G., Kurtz M. J., 1996, AJ, 111, 64
- Matsushita K., Makishima K., Awaki H., Canizares C. R., Fabian A. C., Fukazawa Y., Loewenstein M., Matsumoto H., Mihara T., Mushotzky R. F., Ohashi T., Ricker G. R., Serlemitsos P. J., Tsuru T., Tsusaka Y., Yamazaki T., 1994, ApJ, 436, L41
- Merritt D., 1983, ApJ, 264, 24
- Merritt D., 1984, ApJ, 276, 26
- Nulsen P. E. J., Böhringer H., 1995, MNRAS, 274, 1093
- Oemler A., 1974, ApJ, 194, 1
- Pinkney J., 1995, PhD Thesis, New Mexico State University
- Pinkney J., Rhee G., Burns J. O., Hill J. M., Batuski D., Hintzen P., 1993, ApJ, 416, 36
- Rangarajan F. V. N., White D. A., Ebeling H., Fabian A. C., 1995, MNRAS, 277, 1047
- Raymond J. C., Smith B. W., 1977, ApJS, 35, 419
- Richstone D. O., 1975, ApJ, 200, 535
- Sakelliou I., Merrifield M. R., 1997, in preparation
- Sakelliou I., Merrifield M. R., McHardy I. M., 1996, MNRAS, 283, 673
- chindler S., Prieto M. A., 1997, A&A, accepted for publication
- Scodreggio M., Solanes J. M., Giovanelli R., Haynes M., 1995, 444, 41
- Soltan A., Fabricant D. G., 1990, ApJ, 364, 433
- Stark A. A., Gammie C. F., Wilson R. W., Bally J., Linke R. A., Heiles C., Hurwitz M., 1992, ApJS, 79, 77
- Trinchieri G., Fabbiano G., 1985, ApJ, 296, 447
- van der Marel R. P., de Zeeuw P. T., Hans-Walter Rix, Quinlan G. D., 1997, Nat, 385, 610
- Vikhlinin A., Forman W., Jones C., 1994, ApJ, 435, 162
- White D. A., Fabian A. C., Forman W., Jones C., Stern C., 1991, ApJ, 375, 35
- Wrobel J. M., 1991, AJ, 101, 127